Next Materials 8 (2025) 100564

Contents lists available at ScienceDirect

Next Materials

journal homepage: www.sciencedirect.com/journal/next-materials

Research article

Analysis of artificial intelligence-discovered patterns and expert-designed aging patterns for 0.2 % proof stress in Ni-Al alloys with γ – γ' two-phase structure

Vickey Nandal [a,*,1], Sae Dieb [a], Dmitry S. Bulgarevich [a], Toshio Osada [a], Toshiyuki Koyama [b], Satoshi Minamoto [a], Masahiko Demura [a,*]

[a] National Institute for Materials Science (NIMS), Tsukuba, Japan
[b] Department of Materials Design Innovation Engineering, Nagoya University, Nagoya, Japan

ARTICLE INFO

Keywords:
Artificial intelligence
Monte carlo tree search
Non-isothermal aging
Ni-Al alloys
Pattern analysis

ABSTRACT

This study presents the comprehensive analysis of flexible non-isothermal aging (NIA) patterns discovered through artificial intelligence (AI) to improve the mechanical strength (0.2 % proof stress) in γ – γ' two-phase, binary Ni-Al alloys. In our recent investigation, we found that the AI algorithm could propose aging patterns with superior strength compared to conventional isothermal aging heat treatment. In this current study, we continued our extensive exploration of AI methodologies, uncovering diverse patterns that also surpassed the isothermal aging benchmark. Remarkably, out of 2823 NIA schedules, we found 173 ones outperforming the isothermal aging benchmark. Furthermore, we conducted a detailed analysis of newly AI-discovered patterns and expert-designed patterns inspired by AI. We identified two critical factors for strength improvement: exposure at 700 °C and the number of consecutive 700 °C exposures (optimally set at two), alongside non-consecutive steps (up to five). The insights gained from these findings may demonstrate the potential of AI-driven approaches to yield ideas on how to achieve improved strength in Ni-Al alloys.

1. Introduction

The high-temperature mechanical properties of Ni-based superalloys are finally controlled by the aging heat treatment, which determines the two-phase microstructure consisting of γ' precipitate (gamma prime) and γ (gamma) matrix [1–3] in the system. Currently, the aging treatment of alloys is carried out through conventional isothermal methods [4,5]. However, when examining different alloy systems such as Fe-Cu [6], 2A14 Al [7] Al-Zn-Mg-Cu [8–10], Al-Cu-Mg-Si [11], Al-Zn-Mg [12] and Mg-4Y-2.5Nd-1.2Gd-0.5Zr [13] in the literature, it has been observed that non-isothermal aging (NIA) leads to enhanced mechanical properties compared to the conventional isothermal aging methods. The vastness of the design space for the NIA is a source of possibility, but it also brings with it the difficulty of an exhaustive search. For instance, aging experiments, microstructural observations, and high-temperature mechanical testing are time-consuming and costly, taking about half a month to test a single aging pattern. In fact, due to time and cost constraints, the previous studies on the NIA above-mentioned have limited the search space by confining the freedom of design in aging patterns. Specifically, there is limited research found on the non-isothermal aging of nickel-based superalloys aimed at modifying their two-phase microstructure.

Recently, we have developed a computational workflow that can simulate aging heat treatment and estimate high-temperature strength (i.e., 0.2 % tensile proof stress) for the γ/γ' two-phase microstructure of Ni-Al binary alloys, thereby significantly reducing the time and cost required to test various aging patterns [14]. This computational workflow has been implemented in the material design system named Materials Integration by Network Technology (MInt) [15–18], which was developed at National Institute for Materials Science (NIMS) and allowed users to experiment freely with various aging patterns. By integrating this computational workflow with an AI-based efficient search algorithm, we have succeeded in finding aging patterns that outperform isothermal aging from a vast search space of the NIA in

* Corresponding authors.
E-mail addresses: nandal@fzu.cz, vickeynandal220@gmail.com (V. Nandal), demura.masahiko@nims.go.jp (M. Demura).
[1] Current affiliation: Marie Skłodowska-Curie Actions Postdoctoral Fellow (MSCA-PF), Institute of Physics of the Czech Academy of Sciences (FZU), Na Slovance 2, Prague 182 21, Czech Republic

https://doi.org/10.1016/j.nxmate.2025.100564
Received 20 December 2024; Received in revised form 5 February 2025; Accepted 24 February 2025
Available online 28 February 2025

terms of 0.2 % proof stress at a high temperature. Furthermore, we have proposed a new two-step aging by finding a common principle from the patterns discovered by AI [19].

This study aims to address the limited exploration of the vast NIA design space and the lack of systematic approach into γ' phase evolution (i.e., in terms of optimal size, volume fraction and number density of γ' precipitates) under AI-optimized aging patterns, especially for NIA patterns on Ni-Al alloys. Typically, the size and volume fraction of γ' precipitates play a critical role in determining the yield strength, as demonstrated by Li at al. [20] for Ni-based superalloys. For instance, smaller, finely dispersed γ' precipitates impede dislocation motion more effectively, enhancing strength through precipitation hardening. Additionally, a higher volume fraction of γ' increases the overall barrier to dislocation movement, further elevating yield strength. In this study, specifically, we investigate whether AI-driven methodologies can uncover different superior NIA schedules (i.e., other than our proposed two-step NIA heat treatment route [19]) that enhance the 0.2 % proof stress beyond conventional isothermal aging. We hypothesize that AI-discovered patterns could reveal key thermal exposure factors, such as optimal exposure at 700 ℃ and the role of consecutive and non-consecutive heating steps that contribute to strength improvement.

To achieve this, we systematically explored 2823 NIA patterns suggested by AI, leading to the discovery of various aging schedules surpassing the isothermal aging benchmark. An in-depth analysis of these AI-discovered patterns identified critical factors influencing mechanical strength, particularly the significance of 700 ℃ exposure in aging heat treatment. Additionally, any newly discovered patterns have been categorized within a structured framework to further refine our understanding. This study demonstrates the potential of integrating AI with computational workflows to not only develop superior NIA patterns but also establish important factors that need to be considered for designing optimized aging strategies in Ni-Al alloys. Given the promising results, continued research into NIA scheduling of complex superalloys is expected to be a significant area of interest and investment in the future [6, 12].

2. Computational methods

2.1. Workflow designing for high-temperature strength

In this study, we used the MInt computational workflow to obtain high-temperature strength from aging heat treatments in Ni-Al alloys that we have previously developed [14]. This computational workflow can predict high-temperature strength by modeling microstructure evolution using phase-field simulations throughout the heat treatment process. It comprises three integrated modules: the aging heat treatment simulation module based on phase-field (PF) analysis, the γ' statistic analysis module, and the mechanical property prediction module. These components are incorporated into the MInt system, facilitating the automated calculation of 0.2 % proof stress at any specified high temperature for various heat treatment schedules. Recently, we have reported the usefulness of this computational workflow in proposing two-step aging heat treatment in Ni-Al alloys [19].

The aging heat treatment simulation module can compute the growth of γ' precipitation in the Ni-Al alloy system based on the PF analysis. The detailed of the PF analysis has been reported in [14]. The module outputs the compositional and phase images after a given aging heat treatment pattern. The output file was then automatically transferred to the second module to extract the statistics such as the volume fraction and size of γ' phase and the averaged Al composition in each phase. Based on the statistics, the 0.2 % proof stress (PS) at a high temperature was estimated through an empirical equation counting each contribution of the precipitation hardening, the solution hardening of γ phase, and the strength of γ' phase. The empirical equation has been detailed in [14]. The computed PS value was confirmed to reproduce the experimental one for a certain isothermal aging case in Ni-Al alloys.

2.2. Initial material and search space boundaries

A binary Ni-19.11 at% Al alloy with the γ/γ' two-phase microstructure was the target material in the present study as a model of Ni-based superalloys [3]. The fine γ' precipitates, referred to as secondary γ' precipitates, were the target component of the microstructure. We used the same computational workflow developed [14] for forward prediction of the two-phase microstructure and resulting 0.2 % proof stress at 725 ℃ (i.e., service temperature) and integrated with an AI technique, Monte Carlo tree search (MCTS). In detail, we used the application programming interface of MInt [15–18] to conduct the workflow according to the suggestion by the MCTS and extract the computed result that was fed to the MCTS for rebuilding the [17] searching trees. Herein, we tried to discover new NIA patterns to achieve the outperformed 0.2 % proof stress than the isothermal aging benchmark.

The MCTS algorithm employed coarse-tuned digitalized parameters, precisely the temperature interval, and time step size, to determine the starting temperature for the NIA scheduling. For instance, the starting temperature for the aging temperature input parameter was set within the range of 600 – 800 ℃, with a 50 ℃ interval and a fixed time of 10 minutes (mins). Following the coarse tuning of the starting temperature, the aging temperature range was further considered for fine-tuning to discover the optimal solution. Eventually, during this fine-tuned stage, the possible number of NIA types reached 3,486,784,401. The detailed digitization parameters were reported in our previous report [19]. In this study, they were fine-tuning involved considering a broad range of aging temperatures, spanning from 500 to 700 ℃, with intervals of 25 ℃. The aging schedule was conducted with a fixed time of 10 minutes. It is noteworthy to mention that in the more realistic case of practical Ni-based superalloys, the diffusion coefficient is lower than that of this case. Eventually, the possible controlling time is 10 or 100 times larger than the aging time considered in this study. It is worth emphasizing that aging heat treatment can be tailored according to the complexity of alloys.

2.3. Integration of computational system and AI technique

Fig. 1 illustrates MInt system integration with the AI technique, MCTS, to find the optimal solution to achieve improved 0.2 % proof stress in the Ni-Al alloy system. MCTS (AI technique), a simulation-based approach, was utilized for random sampling to construct trees, enabling intelligent decision-making by estimating the expected value of each possible move. Its popularity can be attributed to its simplicity, scalability, and ability to learn from previous experience [21,22]. In the present study, the input conditions, such as aging temperature, cooling rate, heating rate, and aging time, are fixed by the user and implemented in the computational workflow in the MInt system. The selection of the next aging scheduling is a learned route from the previous schedules by AI.

3. Results and discussion

3.1. Outperformed non-isothermal aging schedules

Fig. 2a displays a schematic illustration of the searching results. It depicts the possible number of heat treatments, including isothermal and non-isothermal aging (NIA) schedules, in a huge search space of 3,486,784,401 (~ 3.5 billion) possibilities. From this search space, the MCTS algorithm proposes a pattern that is likely to outperform the benchmark strength, which is then validated using a workflow implemented in the MInt system. This cycle of proposal and verification was repeated to search for better patterns. In our previous report [19], we carried out 1620 schedules within 12 independent MCTS trees and discovered 110 of them surpassing the isothermal benchmark value.

The previous study [19] inspired us to conduct a more extensive search of NIA schedules with a more significant number of simulations

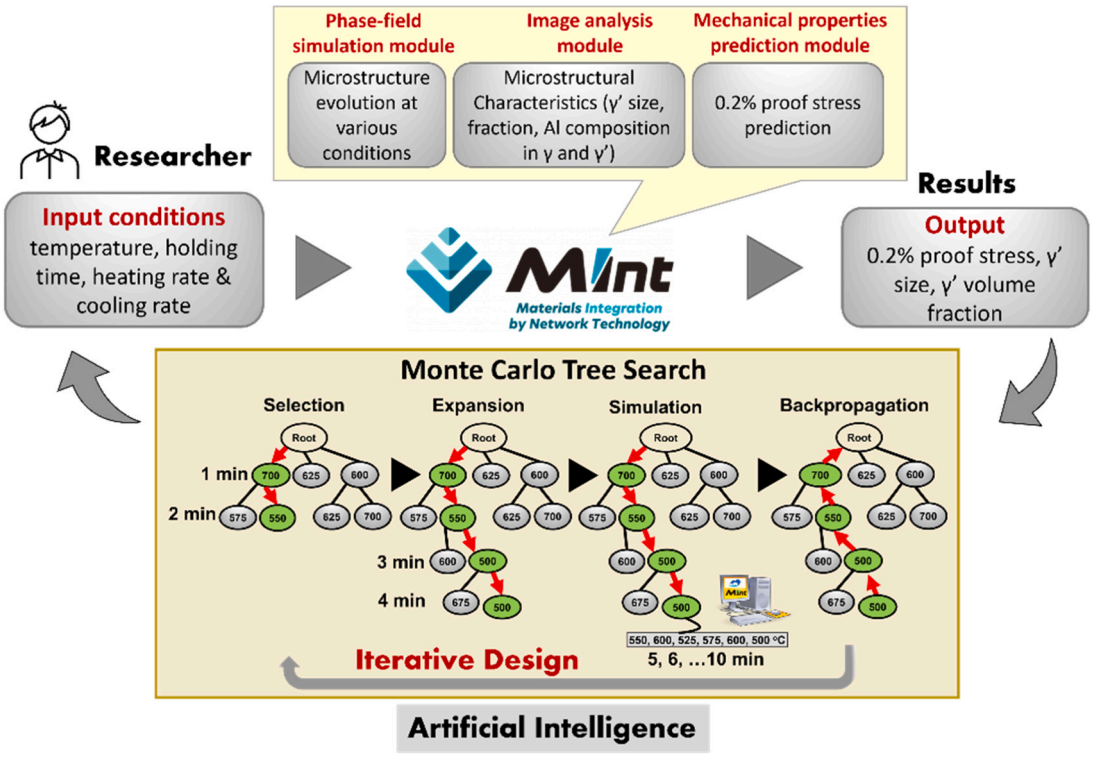

Fig. 1. Computational workflow MInt system, integrating with AI-driven MCTS technique in Ni-Al alloys.

in order to derive rules for constructing patterns that would outperform the benchmark in the Ni-Al alloy. Therefore, in the current study, we performed extensive simulations (for example, 10 more MCTS trees) within the computational budget (i.e., a total of 22 independent MCTS trees) using AI integrated with the MInt system and analyzed the pattern obtained from AI-discovered NIA schedules. Notably, we achieved the NIA design of 63 out of 1203 schedules (i.e., a total 173 out of 2823 NIA schedules), surpassing the isothermal aging benchmark, as illustrated in Fig. 2b and c. The isothermal aging benchmark value (784.5 MPa [19]) is highlighted with a black dashed line (Fig. 2b).

Fig. 2d displays patterns categorized as either outperforming the isothermal aging benchmark (successful) or underperformed (unsuccessful) in relation to the number of 700 ℃ steps, ranging from 1 to 7. It is evident that searching by AI algorithm predominantly favored 1, 2, and 3 no. of 700 ℃ steps. The MCTS algorithm indicates regions with a high probability of achieving outperformed outcomes, prompting a concerted focus on these areas, highlighted by the blue region in Fig. 2d. For instance, out of the 2823 NIA patterns selected by AI, the majority involved 2 numbers of 700 ℃ steps with 110 outperformed cases, as quantified in Table 1. It is important to highlight that surpassing the threshold of 3 steps results in the material undergoing over-aging. Therefore, achieving outperformed cases becomes unattainable when the number of 700 ℃ steps exceeds 3, as determined by the AI design (refer to Table 1). From the above analysis, it is clear that the number of 700 ℃ is one of the important factors in achieving outperformed results.

Upon conducting a more detailed pattern analysis of AI-discovered NIA patterns, we identified another significant contributing factor for surpassing the isothermal aging benchmark. The results indicate that the same number of 700 ℃ steps can yield both outperformed and underperformed cases (refer to Fig. 2b). For instance, when employing 3 steps of 700 ℃, we observed instances of both outperformance and underperformance (as referenced in Table 1). Examples of expert-designed NIA patterns, such outperformed and underperformed cases are presented in Fig. 3.

For instance, the outperformed case involves a sequence of 3 non-consecutive steps at 700 ℃, yielding a 0.2 % proof stress of 785.2 MPa, depicted in Fig. 3a. Conversely, the underperformed case entails 3 consecutive steps at 700 ℃, resulting in a 0.2 % proof stress of 755.2 MPa, as evidenced in Fig. 3b. It is attributed to the substantial increase in the size of γ' and a decrease in their number density in consecutive occurrences, leading to a transition toward the over-aged region, compared to non-consecutive cases, as evidenced in the corresponding phase-field microstructures in Fig. 3. Examining these NIA (non-isothermal aging) patterns elucidates the crucial role of consecutive or non-consecutive step arrangements in achieving outperformed results.

3.2. *Microstructural characteristics*

Generally, the γ' secondary phase is a strengthening phase in these materials to achieve higher mechanical strength [23–28]. In this study, a graphical representation was generated to illustrate the relationship between γ' size and their respective 0.2 % proof stress values derived from approximately 100 NIA patterns identified through AI methodologies, depicted in Fig. 4a. The comparison with the isothermal aging benchmark line (the grey dotted line) shows that the γ' size should be in the 40–42 nm range for achieving outperforming results, as shown by the black dashed line in Fig. 4a, and the ideal size appears to be around 41 nm.

It should be noted that the ideal size of γ' phase can be determined by an anti-phase boundary (APB) energy of 0.10 J/m^2 [19]. The APB energy reported experimentally for stoichiometric Ni_3Al was approximately 0.17 J/m^2 [29]. In other words, γ' sizes below ~ 40 nm signify an under-aged condition, while sizes surpassing ~ 42 nm denote an over-aged state. In detail, the γ' size requirement in the 40–42 nm range is a necessary condition, not a sufficient one. Actually, even within this range, some instances exhibit underperformance compared with the benchmark, potentially attributed to a lower volume fraction of the γ' phase. The phase-field microstructure of three different size ranges (i.e., under-aged, peak-aged and over-aged conditions) is shown in Fig. 4a. In order to further investigate the coarsening behavior of γ' precipitates, the volume fraction and number density of γ' precipitation are analyzed

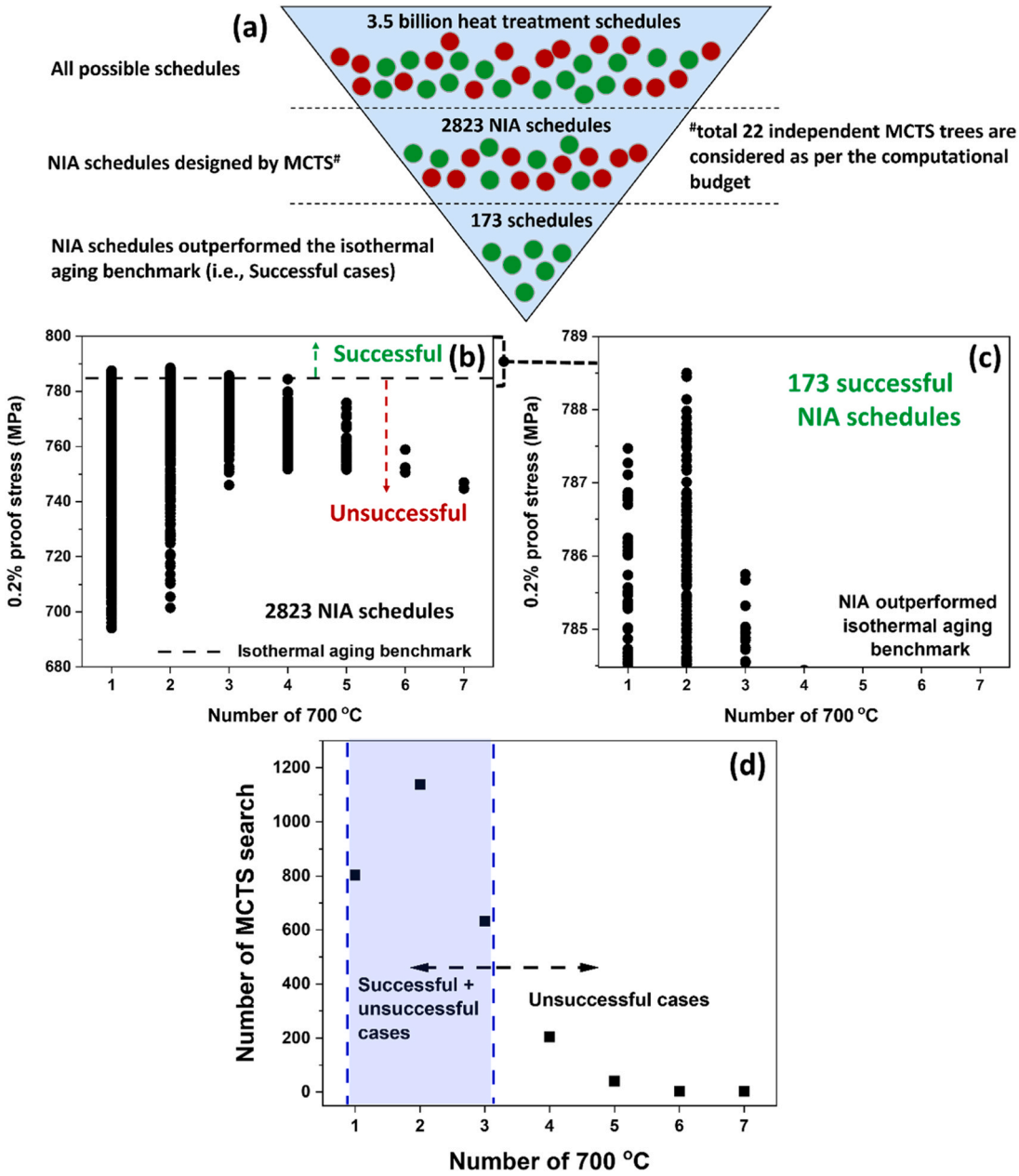

Fig. 2. Plots of (a) provides a schematic representation of the workflow encompassing all heat treatment schedules, (b) showcases the number of NIA schedules discovered by AI, (c) patterns outperformed the isothermal aging benchmark, (d) the number of 700 ℃ versus the number of MCTS search.

Table 1
Outperformed and underperformed cases as a function of 700 ℃ steps discovered by AI.

NIA patterns	Number of 700°C steps			
	1	2	3	4
Outperformed (successful cases)	47	110	16	0
Underperformed (unsuccessful cases)	756	1028	617	204

in a detailed manner for several γ' size ranges in the NIA schedules for both successful and unsuccessful cases. These statistics are presented in Fig. 4b, which illustrate that the number density of precipitates decreases as the γ' size increases from case to case in the NIA schedules. During the aging process, nucleation results in a high number density of γ', but as the precipitates grow, coarsening reduces this density. The larger size of γ' indicates that these precipitates are gradually coarsening (referred as over-aged region), as shown in Fig. 4a. Therefore, a lower number density of γ' is observed (Fig. 4b) in cases where γ' size exceeds 42 nm (Fig. 4a), leading to a decrease in the 0.2 % proof stress. Hence, achieving peak aging, characterized by superior strength, requires an optimal combination of microstructural features, such as size, volume fraction, and number density of γ' precipitates.

3.3. Factors affecting mechanical strength

We identified two crucial factors regarding the scheduling pattern that notably impact the 0.2 % proof stress in Ni-Al alloys. The first factor involves exposure to a temperature of 700 ℃ (refer to Fig. 2b and c), and the detailed analysis suggested that the number of 700 ℃ is not the only factor (refer to Table 1). The second major factor pertains to the consecutive or non-consecutive step arrangement of 700 ℃ (refer to

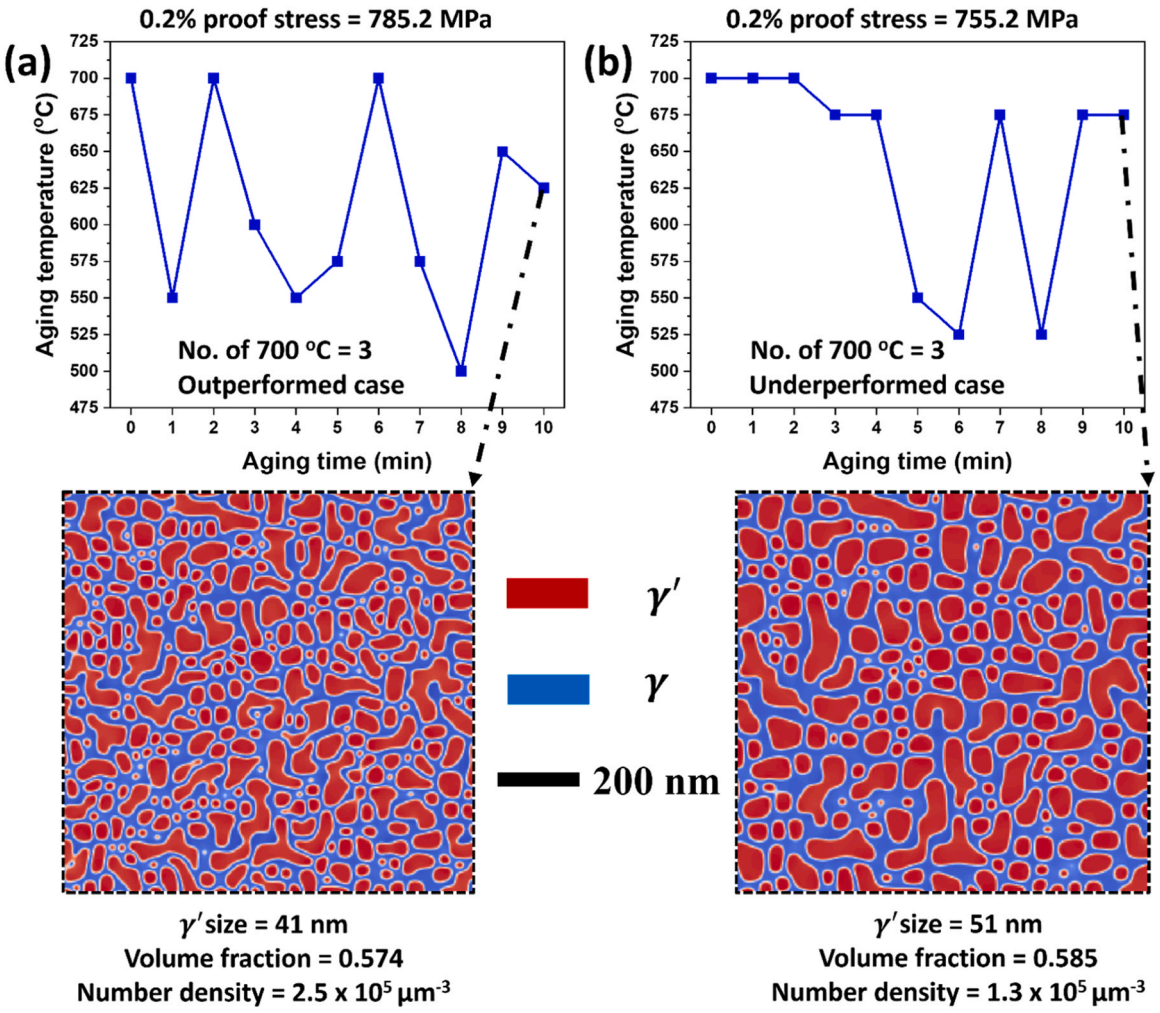

Fig. 3. Typical patterns of (a) outperformed/successful and (b) underperformed/unsuccessful cases of 3 no. of 700 ℃ discovered by AI, corresponding 0.2 % proof stresses and their microstructural features for comparison.

Fig. 3). We here additionally validate the importance of the consecutive or non-consecutive step arrangement through manual virtual experiments (i.e., expert-designed NIA patterns) using the MInt computational system, as shown in Fig. 5. Two manual virtual experiments were carried out, differing in the number of consecutive steps: one with two consecutive steps (orange dotted curve) and the other with three consecutive steps (sapphire dotted curve), as depicted in Fig. 5a. Notably, the optimal scenario for attaining a 0.2 % proof stress was observed with two consecutive steps: initially at 700 ℃ and subsequently reduced to 555 ℃ [19]. However, the aging pattern involving three consecutive steps followed by the lowest considered temperature of 500 ℃ leads to an over-aged state (γ' size ~ 48 nm) and number density of γ' precipitates reduces significantly, consequently resulting in reduced strength compared to the isothermal aging benchmark. Thus, from these observations, we can conclude that the maximum consecutive number of 700 ℃ exposures should not exceed two.

Next, other than number of 700 ℃ exposure, we examine the conditions for the non-consecutive step arrangements. As shown in Table 1, AI found some outperforming patterns, including three steps of 700 ℃; and the preceding conclusion indicates that the 700 ℃ steps in these patterns should be non-consecutive. We conducted a systematic set of virtual experiments for the 3 non-consecutive 700 ℃ steps in Mint computational system, as shown in Fig. 5b; that is, the systematic set of the patterns consisted of the 3 non-consecutive 700 ℃ steps followed by the isothermal steps at various temperatures lower than 700 ℃.

We found that the pattern followed by the isothermal aging at 625 ℃ (i.e., after 3 non-consecutive 700 ℃ steps) outperformed the benchmark value after reaching the near optimal volume fraction, size and number density of γ' precipitates, as illustrated by green symbols in Fig. 5b. Isothermal temperatures below 625 ℃ exhibit an under-aged state where the size of γ' remain below the critical size (approximately 41 nm, see Fig. 4a) and exhibits a lower volume fraction compared to the outperformed case, illustrated by the blue, red, and black curves in Fig. 5b. Similarly, we developed a series of expert-designed NIA patterns for these non-consecutive NIA heat treatments with 4 and 5 steps of 700 ℃, ranging from the highest (700 ℃) to the lowest (500 ℃) considered temperatures, as illustrated in Fig. 5c and d, respectively. For instance, 4 non-consecutive steps, superior outcomes are observed at the subsequent isothermal aging at 600 ℃, as indicated by the yellow symbols in Fig. 5c. Temperatures exceeding this threshold result in an over-aged state, while those below demonstrates an under-aged state.

However, employing a 5-step sequence resulted in an over-aged condition upon subsequent heat treatment exceeding 500 ℃, evident from the increase in γ' size observed at the temperatures, as depicted in Fig. 5d. Hence, among the schedules, only one pattern (the temperature at 500 ℃, indicated by aqua dotted line) could surpass the isothermal aging benchmark. Table 2 illustrates the diverse aging heat treatment sequences, meticulously explored via AI-assisted methodologies and manual investigation, alongside their respective 0.2 % proof stress values, facilitating comprehensive comparative analysis. Importantly, surpassing the 0.2 % proof stress benchmark was unattainable when employing more than 5 non-consecutive steps.

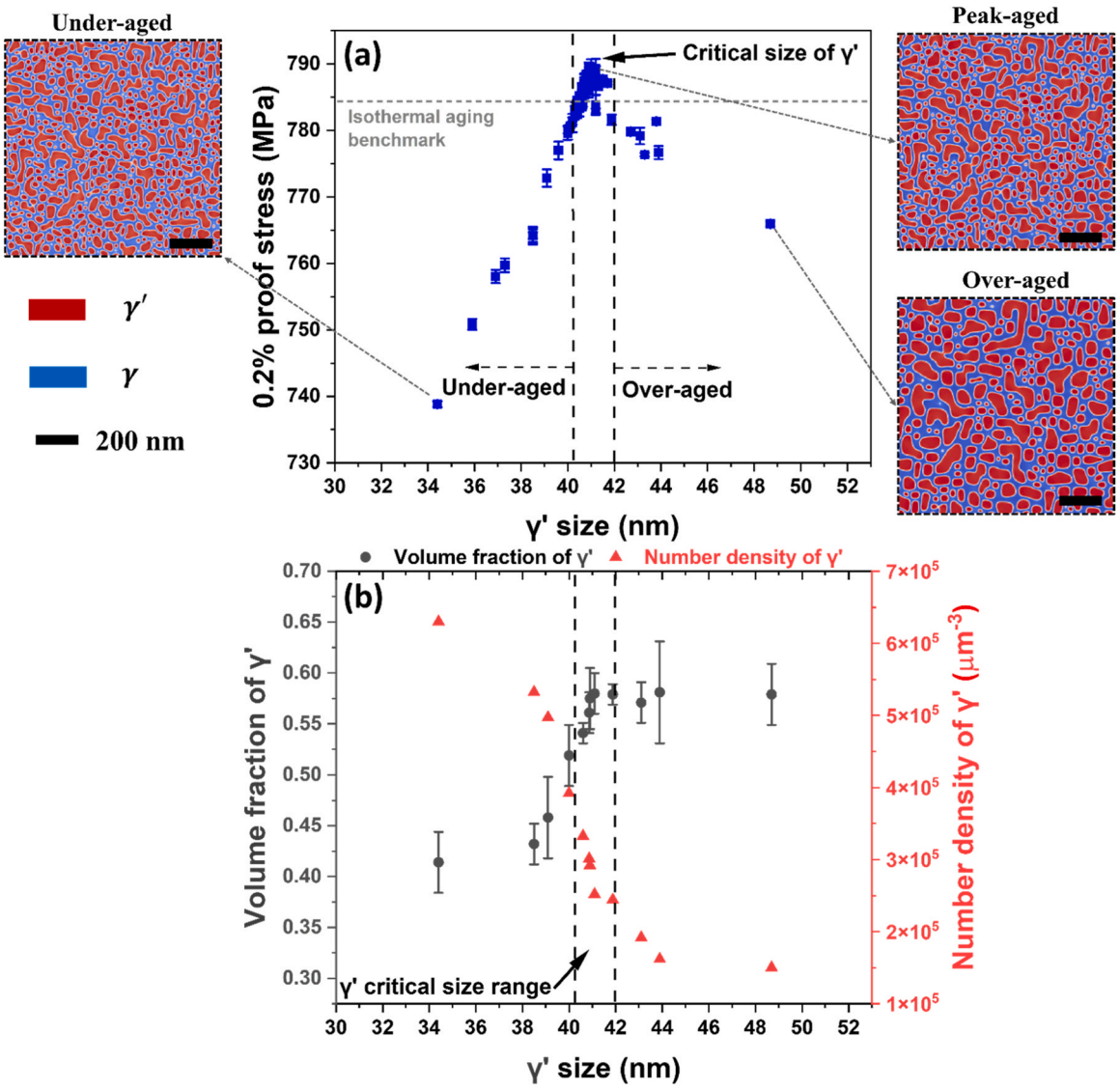

Fig. 4. Plots of (a) 0.2 % proof stress versus γ' size, showing the critical size of γ' and (b) volume fraction and number density of γ' comparing the different range of γ' size in Ni-Al alloy.

Based on the aforementioned observations and analysis, we present a schematic representation of the conditions/rules necessary to achieve an improved 0.2 % proof stress compared to the isothermal aging benchmark in Ni-Al alloys, as depicted in Fig. 6. Two important factors contribute to the improvement of the 0.2 % proof stress. Firstly, subjecting the material to a 700 ℃ step at least once to promote the growth of γ' particles to a size close to the critical threshold (∼ 41 nm). Secondly, the number of consecutive or non-consecutive 700 ℃ steps is critical. The maximum allowable number of consecutive 700 ℃ steps is two; surpassing this limit results in over-aging and a decrease in the 0.2 % proof stress. As for non-consecutive steps, a maximum of five 700 ℃ steps is permissible. Interestingly, through manual heat treatment with insights from AI, we discovered conditions that outperformed conditions for 3, 4 and 5 non-consecutive 700 ℃ steps. It is worth noting that AI could not find the outperforming pattern with 4 or 5 non-consecutive 700 ℃ steps. Overall, consecutive 700 ℃ steps accelerate γ' growth but, if excessive (>2 steps), lead to over-aging and reduced 0.2 % proof stress. On the other hand, non-consecutive steps optimize the γ' phase by balancing growth and coarsening, ultimately leading to improved mechanical properties. Table 3 summarizes the potential for enhancing the 0.2 % proof stress in consecutive or non-consecutive steps.

4. Conclusions

In this study, we discovered overall 173 optimized non-isothermal aging (NIA) schedules designed by AI that outperformed the conventional isothermal aging benchmark in a vast search space of 3,486,784,401 schedules for binary Ni-Al alloys with a γ – γ' microstructure. These NIA schedules revealed two key factors contributing to improvements in 0.2 % proof stress: exposure to 700 ℃ and the nature of consecutive and non-consecutive steps at 700 ℃ temperature. In the context of consecutive thermal treatments at 700 ℃, it is necessary to limit the number of exposures to 700 ℃ to no more than two to prevent rapid growth of the γ' size. In contrast, a series of manually designed non-consecutive NIA heat treatments, encompassing 3, 4, and 5 steps, were established for non-consecutive treatments. These steps spanned the temperature range from the highest (700 ℃) to the lowest (500 ℃) values considered in this study. The 3- and 4-step non-consecutive sequences exhibited notably improved performance, particularly when followed by end temperature heat treatment at 625 ℃ and 600 ℃, respectively. In contrast, 5-step sequences led to over-aging when exposed to treatments exceeding 500 ℃. The outcomes of this study may suggest the feasibility of AI-driven methods in improving the strength of Ni-Al alloys. The variation in the 0.2 % proof stress value in Ni-Al alloy is

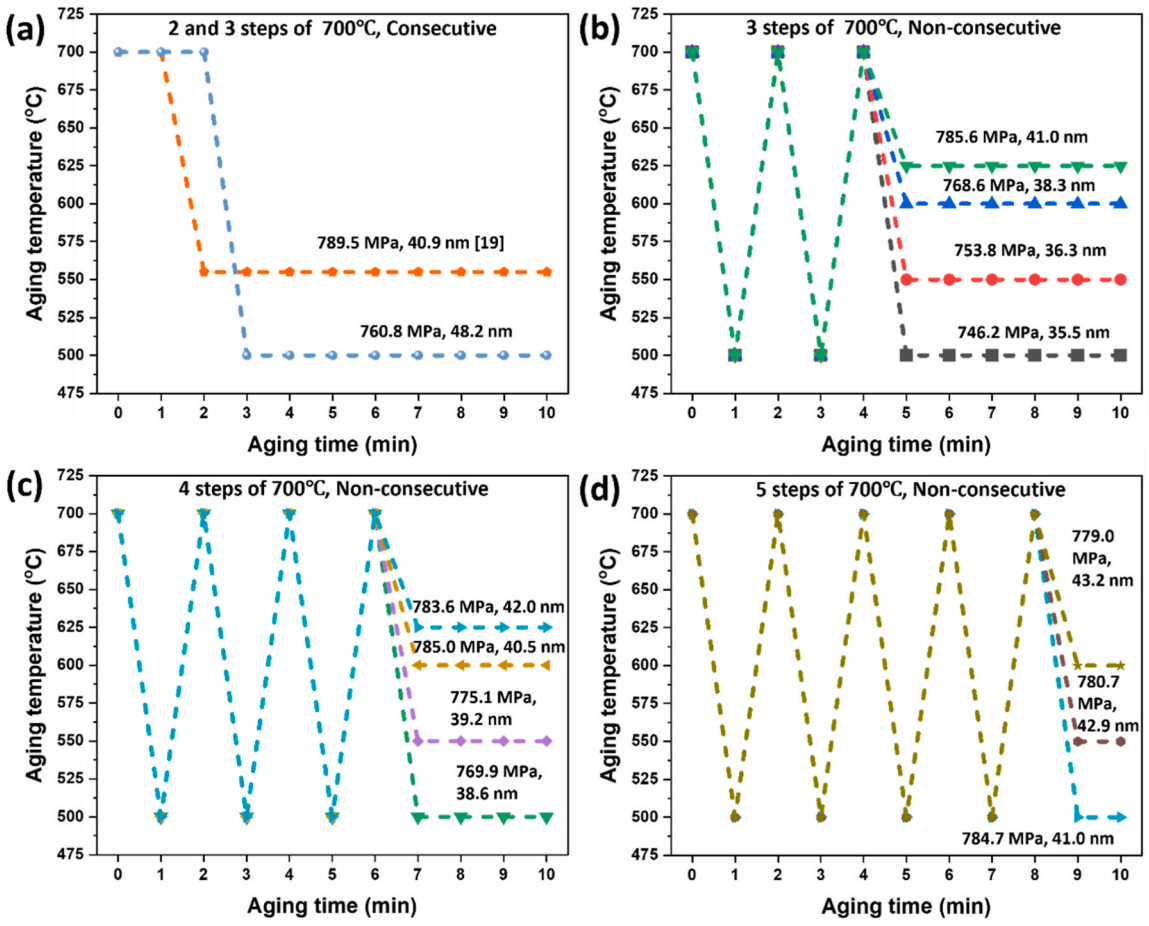

Fig. 5. Graph illustrating the NIA heat treatments designed manually for (a) three non-consecutive 700 ℃ steps, (b) four non-consecutive 700 ℃ steps, (c) five non-consecutive 700 ℃ steps, and (d) two and three consecutive 700 ℃ steps to achieve enhanced strength in terms of 0.2 % proof stress. (Refer to the web version of this article for interpretation of color references in this figure legend).

Table 2
Aging heat treatment schedules discovered by AI and expert-designed, and their corresponding 0.2 % proof stresses.

Aging heat treatment type	Typical pattern	Strength (0.2 % proof stress)
Consecutive (isothermal aging benchmark)	642 ℃ – 10 mins	784.5 MPa
2 consecutive steps of 700 ℃ (maximum strength NIA discovered by AI)	**700** ℃→**700** →550 →500→500→550→600→525→575→600→500 ℃	788.5 MPa
2 consecutive steps of 700 ℃ (expert-designed NIA from AI essence)	**700** ℃→**700**→ 555→555 ℃ (8 mins)	789.5 MPa [19]
3 non-consecutive steps of 700 ℃ by AI	**700** ℃→575→600→600→**700**→625→550→550→**700**→500→600 ℃	785.8 MPa
3 non-consecutive steps of 700 by manual search	**700** ℃→500→**700**→500→**700**→625→625→625→625→625→625 ℃	785.6 MPa
4 non-consecutive steps of 700 by manual search	**700** ℃→500→**700**→500→**700**→500→**700**→600→600→600→600 ℃	785.0 MPa
5 non-consecutive steps of 700 by manual search	**700** ℃→500→**700**→500→**700**→500→**700**→500→**700**→500→500 ℃	784.7 MPa

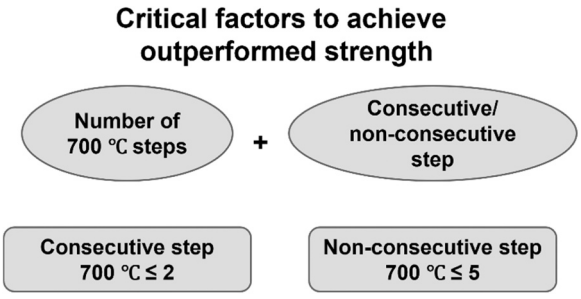

Fig. 6. Critical criteria to follow to surpass the 0.2 % proof stress compared to the isothermal aging benchmark.

Table 3
Aging heat treatment schedules show the potential for enhancing the 0.2 % proof stress in consecutive or non-consecutive cases.

Number of 700 ℃	Consecutive	Non-consecutive	Cases
1	-	Promising	Many
2	Promising	Promising	Major
3	No	Promising	Some
4	No	Promising	Few
5	No	Promising	one
6	No	No	No

minimal. In the future, experimental studies can be conducted to validate these computational findings and confirm the practical effectiveness of the AI-discovered schedules to achieve enhanced mechanical properties. This approach combined with AI can be extended to more complex alloys, such as Ni-Al-Co-based superalloys, to predict their mechanical properties for optimal solutions.

Impact statement

This study uncovers flexible non-isothermal aging patterns using artificial intelligence that surpass traditional isothermal aging methods in γ – γ' two-phase Ni-Al alloys. Among 2823 schedules, 173 exhibit superior strength.

Declaration of Competing Interest

The authors declare that they have no known competing financial interests or personal relationships that could have appeared to influence the work reported in this paper.

Acknowledgements

This work was supported by the Council for Science, Technology and Innovation (CSTI), Cross-ministerial Strategic Innovation Promotion Program (SIP), Structural Materials for Innovation", "Materials Integration" for Revolutionary Design System of Structural Materials (Funding agency: JST) and by MEXT Program: Data Creation and Utilization Type Material Research and Development Project Grant Number JPMXP1122684766. The authors thank the members of the MInt System Team, Materials Data Platform (DPF), NIMS.

References

[1] R.C. Reed, The Superalloys: Fundamentals and Applications, Cambridge University Press, Cambridge, UK, 2006.
[2] A. Kracke, Superalloys, the Most Successful Alloy System of Modern Times-Past, Present, and Future, Superalloys (2010) 13–50.
[3] M. Durand-Charre, The Microstructure of Superalloys, 1st ed., 1968.
[4] V. Nandal, B. Harun, R. Sarvesha, S.S. Singh, Revealing the precipitation sequence with aging temperature in a non-equiatomic AlCoCrFeNi high entropy alloy, Metall. Mater. Trans. A 53 (2021) 314–321, https://doi.org/10.1007/s11661-021-06528-7.
[5] V. Nandal, K. Hariharan, R. Sarvesha, S.S. Singh, Y. Chang, A. Yeh, S. Neelakantan, J. Jain, Aging temperature role on precipitation hardening in a non-equiatomic AlCoCrFeNiTi high-entropy alloy, Mater. Sci. Technol. 37 (2021) 1270–1279, https://doi.org/10.1080/02670836.2021.1996104.
[6] C.R. Hutchinson, M. Gouné, A. Redjaïmia, Selecting non-isothermal heat treatment schedules for precipitation hardening systems: An example of coupled process-property optimization, Acta Mater. 55 (2007) 213–223, https://doi.org/10.1016/j.actamat.2006.07.028.
[7] L. Huang, L. He, S. Chen, K. Chen, J. Li, S. Li, W. Liu, Effects of non-isothermal aging on microstructure, mechanical properties and corrosion resistance of 2A14 aluminum alloy, J. Alloy. Compd. 842 (2020), https://doi.org/10.1016/j.jallcom.2020.155542.
[8] J.T. Jiang, W.Q. Xiao, L. Yang, W.Z. Shao, S.J. Yuan, L. Zhen, Ageing behavior and stress corrosion cracking resistance of a non-isothermally aged Al-Zn-Mg-Cu alloy, Mater. Sci. Eng. A 605 (2014) 167–175, https://doi.org/10.1016/j.msea.2014.03.023.
[9] W. Wang, Q. Pan, X. Wang, Y. Sun, J. Ye, G. Lin, S. Liu, Z. Huang, S. Xiang, X. Wang, Y. Liu, Non-isothermal aging: a heat treatment method that simultaneously improves the mechanical properties and corrosion resistance of ultra-high strength Al-Zn-Mg-Cu alloy, J. Alloy. Compd. 845 (2020), https://doi.org/10.1016/j.jallcom.2020.156286.
[10] D. Jiang, Y. Liu, S. Liang, W. Xie, The effects of non-isothermal aging on the strength and corrosion behavior of Al-Zn-Mg-Cu alloy, J. Alloy. Compd. 681 (2016) 57–65, https://doi.org/10.1016/j.jallcom.2016.04.208.
[11] X. Zhan, J. Tang, H. Li, X. Liang, Y. Lu, Y. Che, W. Tu, Y. Zhang, Effects of non-isothermal aging on mechanical properties, corrosion behavior and microstructures of Al-Cu-Mg-Si alloy, J. Alloy. Compd. 819 (2020), https://doi.org/10.1016/j.jallcom.2019.152960.
[12] M. Nicolas, A. Deschamps, Characterisation and modelling of precipitate evolution in an Al-Zn-Mg alloy during non-isothermal heat treatments, Acta Mater. 51 (2003) 6077–6094, https://doi.org/10.1016/S1359-6454(03)00429-4.
[13] N. Babacan, E. Yurtkuran, A. Balci, M. Bieda-Niemiec, A. Jarzębska, Effects of non-isothermal aging on microstructure and mechanical properties of WE43 alloy, J. Mater. Eng. Perform. 30 (2021) 7909–7916, https://doi.org/10.1007/s11665-021-05977-w.
[14] T. Osada, T. Koyama, D.S. Bulgarevich, S. Minamoto, M. Osawa, M. Watanabe, K. Kawagishi, M. Demura, Virtual heat treatment for γ-γ′ two-phase Ni-Al alloy on the materials Integration system, MInt, Mater. Des. 226 (2023) 111631, https://doi.org/10.1016/j.matdes.2023.111631.
[15] S. Minamoto, T. Kadohira, K. Ito, M. Watanabe, Development of the materials integration system for materials design and manufacturing+ 1, Mater. Trans. 61 (2020) 2067–2071, https://doi.org/10.2320/matertrans.MT-MA2020002.
[16] M. Demura, Challenges in materials integration, Tetsu-to-Hagané (2023), https://doi.org/10.2355/tetsutohagane.TETSU-2022-122.
[17] M. Demura, T. Koseki, SIP-materials integration projects, Mater. Trans. 61 (2020) 2041–2046, https://doi.org/10.2320/matertrans.MT-MA2020003.
[18] M. Demura, Materials integration for accelerating research and development of structural materials, Mater. Trans. 62 (2021) 1669–1672, https://doi.org/10.2320/matertrans.MT-M2021135.
[19] V. Nandal, S. Dieb, D.S. Bulgarevich, T. Osada, T. Koyama, S. Minamoto, M. Demura, Artificial intelligence inspired design of non-isothermal aging for γ–γ′ two-phase, Ni–Al alloys, Sci. Rep. 13 (2023) 12660, https://doi.org/10.21203/rs.3.rs-2593940/v1.
[20] X. Li, Q. Ma, E. Liu, Z. Li, J. Bai, H. Li, Q. Gao, Order phase transition of HIP nickel-based powder superalloy during isothermal aging, J. Alloy. Compd. 1010 (2025) 177269, https://doi.org/10.1016/j.jallcom.2024.177269.
[21] T. M. Dieb, S. Ju, K. Yoshizoe, Z. Hou, J. Shiomi, K. Tsuda, MDTS: automatic complex materials design using Monte Carlo tree search, Sci. Technol. Adv. Mater. 18 (2017) 498–503, https://doi.org/10.1080/14686996.2017.1344083.
[22] T.M. Dieb, S. Ju, J. Shiomi, K. Tsuda, Monte Carlo tree search for materials design and discovery, MRS Commun. 9 (2019) 532–536, https://doi.org/10.1557/mrc.2019.40.
[23] L. Wu, T. Osada, T. Yokokawa, Y. Chang, K. Kawagishi, The temperature dependence of strengthening mechanisms in Ni-based superalloys: a newly re-defined cuboidal model and its implications for strength design, J. Alloy. Compd. 931 (2023) 167508, https://doi.org/10.1016/j.jallcom.2022.167508.
[24] L. Wu, T. Osada, I. Watanabe, T. Yokokawa, T. Kobayashi, K. Kawagishi, Strength prediction of Ni-base disc superalloys: modified γ′ hardening models applicable to commercial alloys, Mater. Sci. Eng. A 799 (2021), https://doi.org/10.1016/j.msea.2020.140103.
[25] T. Osada, N. Nagashima, Y. Gu, Y. Yuan, T. Yokokawa, H. Harada, Factors contributing to the strength of a polycrystalline nickel–cobalt base superalloy, Scr. Mater. 64 (2011) 892–895.
[26] T. Osada, Y. Gu, N. Nagashima, Y. Yuan, T. Yokokawa, H. Harada, Optimum microstructure combination for maximizing tensile strength in a polycrystalline superalloy with a two-phase structure, Acta Mater. 61 (2013) 1820–1829, https://doi.org/10.1016/j.actamat.2012.12.004.
[27] V. Nandal, R. Sarvesha, S.S. Singh, E.W. Huang, Y.J. Chang, A.C. Yeh, J. Jain, S. Neelakantan, Enhanced age hardening effects in FCC based Co1.5CrFeNi1.5 high entropy alloys with varying Ti and Al contents, Materialia 13 (2020), https://doi.org/10.1016/j.mtla.2020.100823.
[28] V. Nandal, R. Sarvesha, S.S. Singh, E.-W. Huang, Y.-J. Chang, A.-C. Yeh, S. Neelakantan, J. Jain, Influence of pre-deformation on the precipitation characteristics of aged non-equiatomic Co1.5CrFeNi1.5 high entropy alloys with Ti and Al additions, J. Alloy. Compd. 855 (2021) 157521, https://doi.org/10.1016/j.jallcom.2020.157521.
[29] T. Kruml, B. Viguier, J. Bonneville, J.L. Martin, Temperature dependence of dislocation microstructure in Ni3(Al,Hf), Mater. Sci. Eng. A 234–236 (1997) 755–757, https://doi.org/10.1016/S0921-5093(97)00391-2.